

ON THE CHARACTERISTICS OF SAND WAVES FORMED UPON THE BEDS OF THE OPEN CHANNELS AND RIVERS

SHINOHARA, Kinji
Research Institute for Applied Mechanics, Kyushu University

TSUBAKI, Toichiro
Research Institute for Applied Mechanics, Kyushu University

<https://doi.org/10.5109/7162488>

出版情報 : Reports of Research Institute for Applied Mechanics. 7 (25), pp.15-45, 1959. 九州大学応用力学研究所
バージョン :
権利関係 :



ON THE CHARACTERISTICS OF SAND WAVES FORMED UPON THE BEDS OF THE OPEN CHANNELS AND RIVERS

By Kinji SHINOHARA and Tōichirō TSUBAKI

In our preceding paper, we have studied the scale of sand waves in connexion with their influences on the characters of flow and of sand transport. In the present report, we are concerned with the same problems again, but on the more extensive experimental basis. At first, introducing a practical parameter which represents the effect of sand waves on the rate of sand transport, the formula of sediment load is derived. Next, the scale, the advance velocity, etc. of the sand waves are discussed with reference to the hydraulic conditions of the flow and the bed materials, and it is pointed out that the characters of sand waves are fairly different according as the grain diameter of sands composing the bed, corresponding to the modes of movement. Further, it is made clear that there exists a close correlation between the equivalent roughness of the flow and the scale of sand waves, and making use of these results, some considerations are shown on the law of resistance in the rivers with sand transport.

1. Introduction. It is a commonly observed fact that the sand waves develop on the movable beds of open channels and rivers. These waves of sands have been early noticed with much interest, but remain as a puzzling problem even now. G. K. Gilbert [1] has pointed out that there exist two kind of sand waves corresponding to the water velocity, and has referred to the one which moves downstream as a 'dune', while the other which moves upstream against the flow as an 'antidune'. Exner [2] has shown theoretically that if a mound is supposed to be given on the bed, then it tends to deform into a certain asymmetrical shape having the gentle slope in the rear side and the steep slope in the lee side, like as the profile of dune. Recently, A. G. Anderson [3] has obtained an expression for the ratio, wave-length/flow-depth, regarded as a function of the Froude number, basing on the idea that the velocity oscillations near the bed induced by the surface waves in the stream cause the variations of sand transportation rate along the bed, which in turn result in the formation of bed undulations.

H. K. Liu [4], on the other hand, has carried out the experiments of determining whether the sediment ripples are caused by surface waves or not, and has found that the surface waves are not the primary cause of sediment ripples. He has suggested that the ripple formation is a phenomenon associated with the instability of the interface, i.e. the transition layer between the fluid and the bed. In these lines of thought, Liu has succeeded in obtaining a criterion for the ripple formation, but the height and length of the ripples have been left undetermined.

At any rate, it is evident that the flow of the stream near the bed and the movement of the sand must be largely influenced by the sand wave, so long as

they exist. In fact, according to the recent studies, the appearance of the sand wave is followed not only by the remarkable increase of the flow resistance but by the decrease of the rate of the transportation under the equal tractive force. We must say, however, the subjects have not been exhausted altogether in the sense that these studies are solely concerned with the measurements of the stream velocity or those of the transportation rate only without referring to the sand wave itself.

Up to now very little has been reported on the observations of sand wave, and hence the author's present information about it is too scarce to sketch their complex characters. Accordingly, the first step to clarify these problems must be to describe the characters of the wave, especially the wave-length, the wave-height and the advance velocity, etc., in terms of the hydraulic conditions of the flow and the bed materials quantitatively. Then the second step is to find out the influences of sand wave upon the sediment transport theoretically and experimentally, basing on the simultaneous observations of the sand waves, the velocity of flow and the rate of transportation.

Thus, as a continuation to the preceding paper [5] in which some contributions to these problems were made through the experiments in the large-scale channels along the Hii River, the authors have attempted to collect the systematic data through the observations at the Hii River itself and the flume experiments with fine sand. In this report, the characters of the sand waves and their influences upon the sand transport are discussed on the basis of the extensive experimental results, including those of the former investigators as well as the ours.

2. Methods of observations.

(a) Observations at the Hii River.

The Hii River is a typical example of sand laden river in Japan, and its



Photo. 1. Channels along the Hii River.

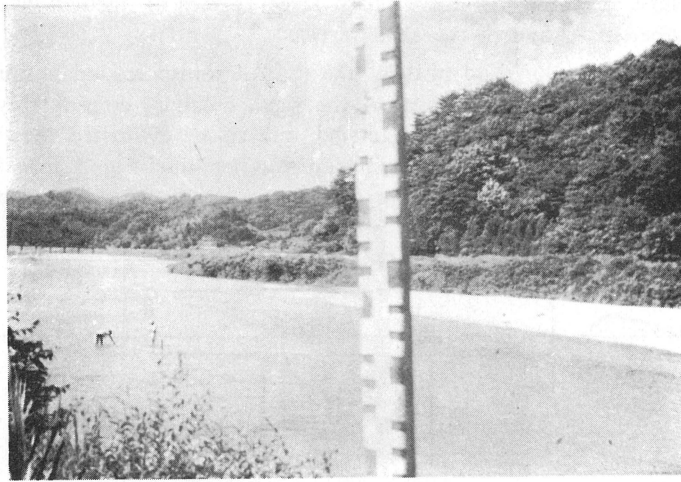


Photo. 2. The Hii River. (Igaya)

bed is covered with beautiful sand waves. Succeeding the former observations of sand waves in the large-scale channels (Photo. 1) along the river, the authors conducted in 1954 the field observations concerning sand waves, the flow characteristics of the stream and the rate of transportation like before. The stations were located at Nadabun, Kurihara and Igaya, about 4 km, 13 km, 26 km distant from the river mouth respectively (Photo. 2).

The methods of measurements are essentially similar to those described in the preceding paper, but in view of the fairly remarkable local variations of the flow-depth, the direction and the magnitude of the stream velocity, etc. some alterations were made for the case of this natural river. That is, in order to avoid the effects of these irregularities, we stretched in the flow-direction a rope 20~30 m long, at the middle of which the measurements of sand transport were to be made. And the wave-length λ , the depths of water h_r at the trough, and h_v at the crest, were directly measured for each individual wave. Thus, by averaging them the wave-height H and the wave-length λ corresponding to the hydraulic condition *as a whole* were determined. To find the surface slope, the difference of the surface levels was measured for the distance of 20~30 m along the rope, making use of the static tube together with the inclined manometer of three enlargement. The measurements of velocity distribution were carried out by means of the current meter of propeller type (3 cm in outer diameter).

In reality, each individual sand wave is never uniform in its scale, but has somewhat irregular shape. In order to examine the degree of fluctuations in this case, we calculated the mean values \bar{x} and the standard deviations σ from the observed data with the result that the mean value of $\frac{\sum \sigma}{N} \bigg/ \frac{\sum \bar{x}}{N}$ for the wave-height, the wave length and the advanced velocity were 0.39, 0.26 and 0.19, respectively. Since these values are nearly equal to those obtained in the channels

of regular shape, it seems that these fairly large degrees of fluctuations are nothing but an inherent feature of the sand waves.

In the presence of sand waves, the rate of transportation is minimum at the trough and maximum at the crest of the wave, changing considerably between them along the gentle slope of the rear side, and so we evaluated the bed load from the quantities collected by the bed load sampler like Fig. 1 in a full wave length. Two conditions are required for this apparatus: firstly, the bottom of con-

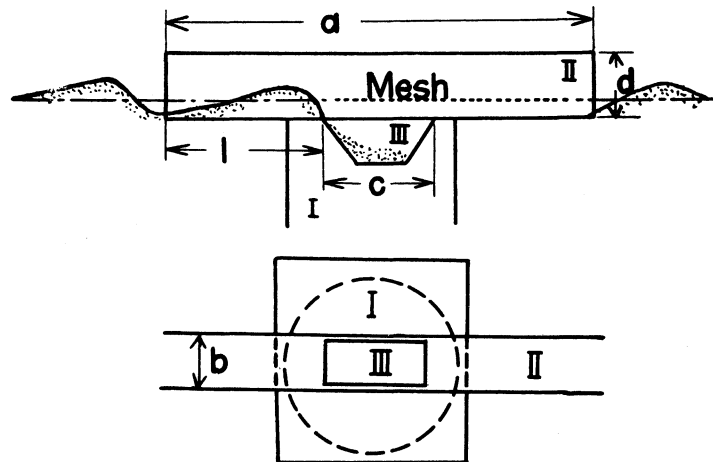


Fig. 1. Bed load sampler. (The Hii River)

duit (II) should be laid lower than the trough of sand waves, and secondly, the length l in Fig. 1 should be large enough to avoid the influence of the step formed near the bucket (III), for the moving grains tumble down in stratum to the bucket along the steep slope, which nearly corresponds to the repose angle of sand.

In the present work, we have prepared three kinds of bed load sampler, whose dimensions are shown in Tab. 1, together with the fourth which had been used in the channel measurements before (Fig. 3 of the preceding paper,) but in

Table 1. Dimensions of bed load sampler (cm)

type	a	b	c	d	l
L	200	50	80	50	75
M	120	30	60	30	40
N	40	10	10	10	20

the river measurements the sampler of medium size (M) was mainly used. By the way, for the purpose of comparing the performances of these samplers, simultaneous observations were made in the channel of $200\text{ m} \times 8\text{ m}$ (length \times width) locat-

ed at Kurihara, setting the three samplers, i.e. M , N , and for channel use. in parallel. We conducted these tests ten times for various values of discharge; it was known that the mean ratio of the transportation rate obtained by the sampler M to those by N was 1.05, indicating no appreciable difference between the performances of these two samplers. But the ratio of the transportation rate obtained by

the sampler M to those by the sampler for channel use was 1.60 in the mean. This value must be attributed to the fact that l of the latter sampler is too short (corresponding to $l=5$ cm) to prevent the scour of the bed near the intake, about which the surrounding sand grains gather together. Therefore, the observed values of the transportation rate in the channels were corrected by this amount.

The procedures of the observations in the Hii River were as follows: first of all we measured the scales of sand wave, and then proceeded to the measurements of the transportation rate where we were concerned with the typical wave having the length and the height which were nearest to the mean values appropriate for that hydraulic condition of the flow. As these procedures called for

considerable time to be carried out, the surfaces slope and the stream velocities were measured during the transport measurements. Incidentally, the specific weight of the bed materials was 2.65, and Fig. 2 shows its cumulative frequency diagram. The results of these observations together with those in the large scale channels are summarized in Table 2, where the following notations are to be understood.

$h = \frac{h_v + h_T}{2}$: arithmetic mean of the water depths at the crest and at the trough

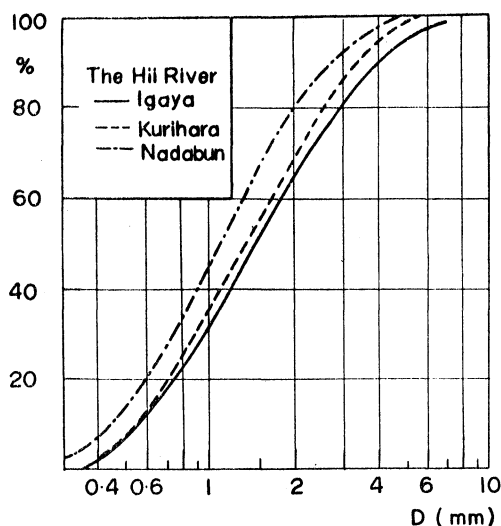


Fig. 2. Cumulative frequency diagram of the bed materials in the Hii River.

I : surface slope

\bar{u} : mean velocity of flow

H : wave height

λ : wave-length

u_r : advanced velocity of sand wave

q : rate of transportation in volume of material per unit time, per unit width of cross section

$u_* = \sqrt{ghI}$: shear velocity

s : specific weight of sand in water

D : grain diameter of sand

$\Psi = \frac{u_*^2}{sgD}$: dimensionless representation of tractive force acting on the grain. When the bed is composed of sand mixture, median diameter D_{50} is used in this report.

$\varphi = \frac{\bar{u}}{u_*}$: denoting Chézy coefficient by C , $\varphi = \frac{C}{\sqrt{g}}$

Table 2. Results of observations in the Hii River* and large scale channels**

h	$I \times 10^3$	\bar{u} (cm/sec)	H (cm)	λ (cm)	u_r (cm/sec)	q (cc/cm.sec)	u_* (cm/sec)	Ψ	φ	$\Psi \frac{\varphi}{\varphi_0}$	$\frac{H}{\lambda}$	$\frac{H}{h}$	$\frac{u_r h}{\sqrt{sgD^3}}$	Φ
①	②	③	④	⑤	⑥	⑦	⑧	⑨	⑩	⑪	⑫	⑬	⑭	⑮
Igaya, the Hii river $D_{50} \div 1.44$, $D_{65} \div 2.05$ (mm)														
20.8	1.15	58.0	1.45	79.5	0.169	—	4.84	0.0919	12.13	0.0691	0.0182	0.0697	1.48	—
24.3	0.898	59.5	1.50	64.0	0.137	—	4.62	0.0911	12.88	0.0653	0.0234	0.0618	1.50	—
28.7	0.964	59.0	1.70	77.0	0.131	—	5.20	0.112	11.35	0.0691	0.0221	0.0592	1.63	—
30.7	0.840	72.5	3.0	112	0.098	0.102	5.03	0.110	14.41	0.0845	0.0270	0.0980	1.27	0.048
32.4	1.06	59.2	3.2	96.0	0.087	—	5.81	0.124	10.19	0.0664	0.0333	0.0988	1.03	—
39.7	1.06	74.2	3.0	124	0.109	0.186	6.43	0.153	11.54	0.0919	0.0240	0.076	1.59	0.068
42.5	0.85	71.3	5.1	138	0.092	0.133	5.94	0.146	12.00	0.0897	0.037	0.120	1.76	0.058
49.3	0.86	70.1	6.8	139	0.073	0.152	6.51	0.179	10.77	0.0970	0.049	0.138	1.61	0.068
59.0	0.88	74.1	8.5	179	0.104	0.494	7.13	0.240	10.39	0.123	0.048	0.144	3.22	0.260
65.2	1.48	93.0	9.4	234	0.101	0.621	9.72	0.400	9.57	0.183	0.040	0.144	2.94	0.277
69.9	1.01	80.1	8.1	134	0.105	0.325	8.32	0.326	9.63	0.152	0.060	0.116	3.85	0.171
73.2	1.53	80.7	13.8	284	0.070	0.425	10.47	0.466	7.71	0.173	0.056	0.188	2.31	0.192
Kurihara, the Hii River $D_{50} \div 1.33$, $D_{65} \div 1.82$ (mm)														
20.2	1.66	70.0	4.2	120	0.151	0.295	5.73	0.158	12.22	0.109	0.036	0.206	1.66	0.160
37.2	1.38	75.2	7.5	159	0.100	0.219	7.10	0.207	10.59	0.110	0.047	0.202	1.59	0.094
38.7	0.89	63.0	6.1	112	0.085	0.125	5.87	0.179	10.73	0.0992	0.055	0.158	1.99	0.076
45.4	1.42	80.3	6.2	119	0.152	0.230	7.95	0.304	10.10	0.125	0.052	0.137	3.74	0.125
Nadabun, the Hii River $D_{50} \div 1.10$, $D_{65} \div 1.46$ (mm)														
70.5	1.53	78.8	25.0	213	0.050	—	10.28	0.599	7.67	0.211	0.117	0.360	2.40	—
84.8	1.53	88.5	22.4	276	0.093	—	11.27	0.709	7.85	0.254	0.081	0.264	5.35	—
87.7	1.42	89.2	17.4	226	0.094	—	11.05	0.681	8.07	0.250	0.077	0.199	5.61	—
103.3	1.53	89.6	25.2	287	0.109	—	12.44	0.864	7.20	0.276	0.088	0.244	7.74	—
Channel A, (2.0 m. width) $D_{50} = 1.26$, $D_{65} = 1.68$ (mm)														
15.6	1.69	58.0	2.85	120	0.126	0.101	5.08	0.126	11.40	0.084	0.0237	0.182	1.09	0.056
18.6	1.73	—	2.73	116	0.109	0.185	5.61	0.154	—	—	0.0235	0.147	1.13	0.103
19.8	1.61	62.6	2.27	106	0.132	0.133	5.59	0.152	11.20	0.095	0.0209	0.112	1.45	0.0734
24.9	1.63	68.6	3.27	114	0.101	—	6.30	0.194	10.89	0.115	0.0286	0.131	1.40	—
25.7	1.61	67.0	4.97	136	0.099	0.179	6.36	0.198	10.53	0.112	0.0366	0.194	1.41	0.0989
29.2	1.67	73.4	5.93	138	0.103	0.229	6.91	0.233	10.62	0.131	0.0431	0.204	1.66	0.127
34.4	1.66	75.8	6.68	150	0.089	0.239	7.48	0.273	10.13	0.143	0.0445	0.194	1.70	0.132
35.5	1.66	70.6	6.40	147	0.093	—	7.59	0.281	9.28	0.135	0.0434	0.180	1.83	—
46.7	1.66	76.5	8.26	158	0.101	0.326	8.72	0.371	8.77	0.162	0.0524	0.177	2.61	0.181
Channel B, (0.8 m. width) $D_{50} = 1.26$, $D_{65} = 1.68$ (mm)														
10.8	1.69	54.9	1.02	105	0.141	0.0504	4.22	0.087	13.00	0.0696	0.0097	0.095	0.838	0.0279
14.5	1.72	60.3	1.54	83	0.124	0.0418	4.94	0.119	12.22	0.0852	0.0186	0.107	0.996	0.0234
14.8	1.75	—	2.35	106	0.103	—	5.04	0.124	—	—	0.0221	0.158	0.845	—
15.7	1.65	—	1.65	93	0.092	0.0656	5.04	0.124	—	—	0.0177	0.105	0.799	0.0364
17.3	1.66	61.6	1.95	91	0.096	—	5.31	0.138	11.60	0.0920	0.0213	0.112	0.917	—
23.1	1.61	63.0	2.95	87	0.132	—	6.03	0.177	10.45	0.101	0.0324	0.127	1.69	—
30.7	1.64	68.4	7.02	129	0.082	—	7.02	0.241	9.74	0.124	0.0545	0.229	1.40	—
Channel C, (2.0 m. width) $D_{50} = 1.46$, $D_{65} = 1.96$ (mm)														
29.5	1.37	66.1	5.60	127	0.071	0.163	6.30	0.167	10.49	0.0944	0.0441	0.190	0.922	0.0722
35.8	1.40	69.0	6.38	150	0.054	0.196	7.00	0.207	9.85	0.0877	0.0434	0.178	0.845	0.0871
35.9	1.46	74.0	5.40	134	0.078	0.271	7.16	0.216	10.34	0.118	0.0406	0.151	1.23	0.120

* As the local variations of grain size in the Hii River have been found, Ψ , Φ etc. in Tab. 2 are calculated from the values of D_{50} at the places where each measurement of sand transport has been done.

** The data in the preceding paper are reproduced with corrected q .

$\phi = \frac{q}{\sqrt{sgD^3}}$: intensity of the transportation rate.

(b) Measurements in the flume experiments with fine sand.

The experiments were performed making use of the wooden channel of 5.5 m in length, 34.6 cm in width equipped in the Department of Civil Engineering, Faculty of Engineering, Kyūshū University. The bed of the flume was covered by

a sand layer of 10 cm thick, which was composed of almost uniform grains of 0.21 mm in D_{50} . Fig 3 shows the cumulative frequency diagram of the sand, the specific weight of which was 2.65.

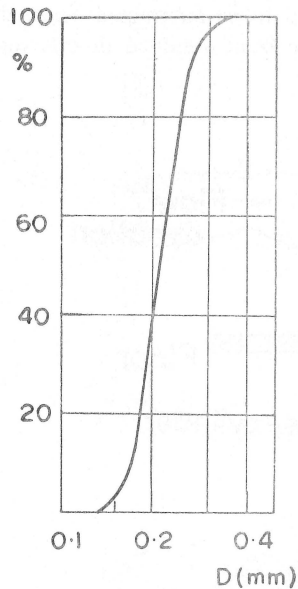


Fig. 3. Cumulative frequency diagram of fine sand.

Once the bed materials set in motion under the action of the running water, the bed which has been even and flat at the outset becomes unstable, and the small two-dimensional sand waves appear at once. In the beginning, they resemble in shape those observed at the Hii River, but as the time elapses, they tend to deform into the complicated appearances with increasing height and roundness at the crest (see Photo. 3). The observations of sand wave were made through the glass window of 80 cm long at the middle parts of the flume by taking the photograph or by reproducing several times, the silhouettes of sand waves as well as of surface waves on the sheets of tracing paper attached on the window glass.

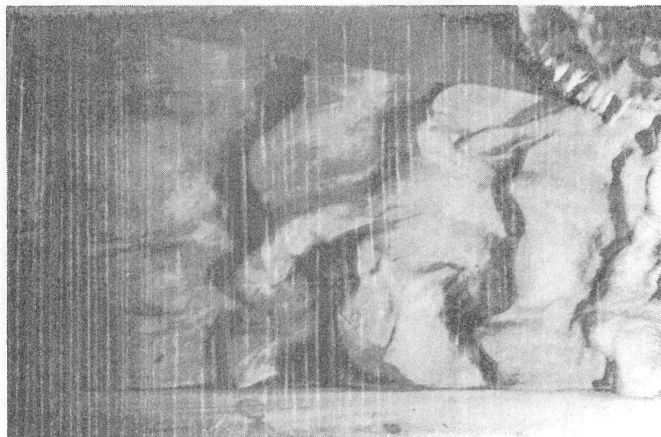


Photo. 3. Profile of sand waves. (fine sand)

Fig. 4 shows the use of the sediment sampler in practice. The moving sand, which passes through the sampling hole 1.7 cm distant from the intake, is lead to a meas-cylinder (1 liter), while most of the suspended load are sedimented in the vessels II and III. But as the sand through I will contain a certain fraction of the suspended load besides the bed load, the sediment sampler with a number of similar small chambers of 2 cm long (Photo. 4) is used for the purpose of separating the bed load from the total load. Namely, observing the distribution of the suspended load sedimented in each of these chambers, and extrapolating it, the amount of suspended load through I can be estimated to be subtracted from the total load. The values in the column 8 of the table have been obtained in this way.

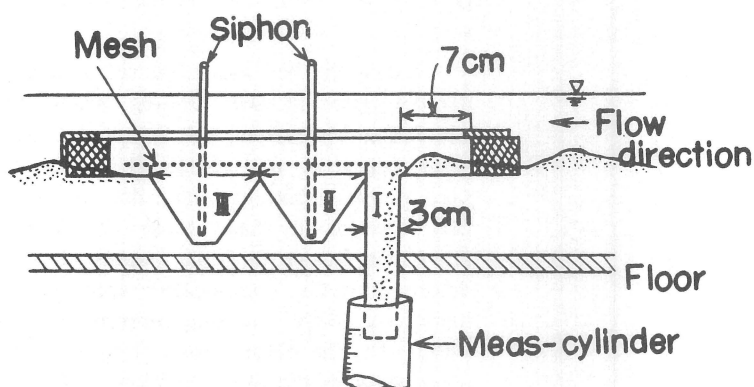


Fig. 4. Sediment sampler.

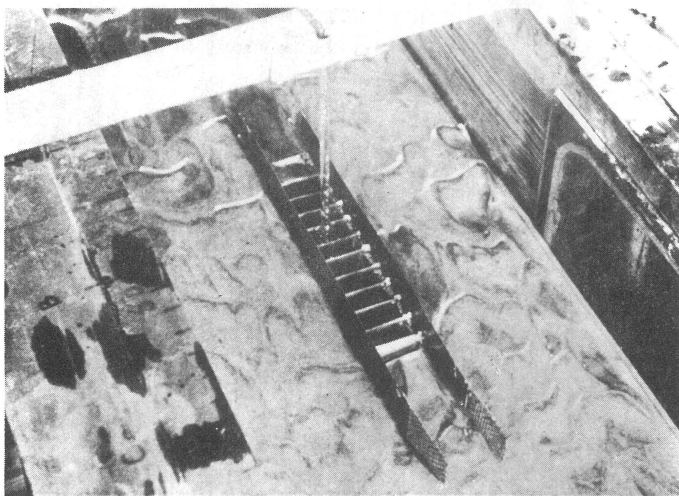


Photo. 4. Sediment sampler for separating the bed load from total load.

The results obtained are summarized in Table 3. In this table, the flow depth has been calculated from the area of the running water, and I in the col-

umn 2 means the energy slope defined by

$$I_e = I_w + \left(I_b - I_w \right) \frac{\bar{u}^2}{gh}$$

where I_w and I_b denote the slope of surface and of bed respectively. The scales of sand waves are determined by averaging over the measurements for individual wave. To eliminate the effects of side wall, the hydraulic radius of bed R_b is calculated by the following Einstein's formula [6] :

$$R_b = h \left(1 - 2 \frac{R_w}{b} \right), \quad R_w = \left(\frac{n_w \bar{u}}{\sqrt{I_e}} \right)^{1.5} \quad (m. sec. unit)$$

where the Manning's n_w of the side wall has been considered as 0.01. In the column 10, u_* means the shear velocity of bed and is defined by $u_* = \sqrt{g R_b I_e}$.

3. Influences of sand waves upon the transportation rate. H. A. Einstein [7] explained the decrease of the transportation rate in the presence of sand waves by postulating that the total resistance of flow consists of two parts: (1) a part depending on the roughness of the sand grains, and (2) a part resulting from the pressure difference between the lee side and rear side of the sand wave, and it is not the total resistance but only the former part of it which is of great importance for the bed load movement. According to him, the resistance τ' and the hydraulic radius R' due to the sand grains are given by the following formula :

$$\tau' = \rho g R' I$$

$$\frac{\bar{u}}{\sqrt{g R' I}} = 5.75 \log_{10} \left(12.27 \frac{R' x}{D_{65}} \right) \quad \} \quad (1)$$

where ρ is the density of water and x means a correction factor for the departure from the rough region. It is true that this idea of Einstein is quite an epoch-making one, and as its results the previous theory in which the bed load has been expressed in terms of the total resistance are compelled to be largely altered. Nevertheless, it seems to the authors that there remain some questions yet on the physical background of his composite roughness and on the accuracy of the Eq. (1) as well.

In this section, let us seek for a practical formula of the sediment transportation rate, introducing the parameter which represents the effect of bed irregularity, but without entering into the hydraulic mechanism, the considerations of which are reserved for the subsequent paper.

Fig. 5 shows the relation between the intensity of transportation rate near the bed* Φ and the dimensionless tractive force Ψ , where use is made of the experimental results of the former authors and of the present authors. In the absence of sand waves, Φ is related to Ψ only. The curves T and E in Fig. 5 correspond to this special case; the curve T represents the equation previously obtained by one of the authors [8]

* The physical meanings of this load are discussed in the Appendix.

Table 3. Results of experiments. (0.21 mm sand)

h (cm)	$I \times 10^3$	\bar{u} (cm/sec)	H (cm)	λ (cm)	u_r (cm/sec)	q (cc/cmsec)	q_b (cc/cm sec)	R_b	u_* (cm/sec)	ψ	φ	$\psi \frac{\varphi}{\varphi_0}$	H/λ	H/R_b	$\frac{u_r R_b}{\sqrt{sgD^3}}$	ϕ
①	②	③	④	⑤	⑥	⑦	⑧	⑨	⑩	⑪	⑫	⑬	⑭	⑮	⑯	⑰
1.89	8.09	14.4	1.10	18.0	0.0154	0.0095	0.0076	1.89	3.91	0.450	3.70	0.099	0.061	0.583	0.242	0.079
2.20	11.30	19.1	1.20	20.0	0.033	0.031	0.0166	2.17	4.89	0.704	3.91	0.159	0.079	0.553	0.595	0.255
2.48	10.70	23.2	1.26	22.2	0.236	0.072	0.032	2.42	5.05	0.751	4.59	0.197	0.057	0.521	3.04	0.597
2.61	9.75	18.6	0.72	14.6	0.052	0.043	0.0178	2.57	4.95	0.721	3.76	0.153	0.050	0.300	1.19	0.358
2.80	9.27	25.2	1.47	23.8	0.100	0.046	0.0152	2.73	4.98	0.731	5.06	0.208	0.062	0.540	2.19	0.370
3.08	8.04	28.4	0.94	15.5	0.130	0.161	0.074	2.98	4.84	0.690	5.86	0.224	0.061	0.316	3.26	1.34
3.20	7.28	40.5	0.77	16.1	0.267	0.209	0.123	3.01	4.63	0.633	8.75	0.307	0.048	0.256	6.61	1.73
3.37	8.39	46.3	0.46	15.3	0.370	0.332	0.163	3.15	5.09	0.762	9.10	0.380	0.030	0.147	9.58	2.76
3.62	7.08	35.1	0.70	13.0	0.172	0.170	0.090	3.44	4.88	0.702	7.19	0.274	0.054	0.202	4.91	1.42
3.71	6.69	50.6	0.41	11.5	0.350	0.231	0.134	3.38	4.71	0.651	10.72	0.381	0.036	0.121	7.81	1.92
3.87	6.44	55.6	0.21	16.0	0.270	0.351	0.193	3.46	4.71	0.654	12.02	0.427	0.013	0.061	7.81	2.92
3.41	5.82	31.1	1.28	22.0	0.072	0.050	0.028	3.24	4.30	0.543	7.23	0.214	0.058	0.375	1.94	0.413
4.23	5.82	35.0	1.35	18.9	0.108	0.074	0.039	3.99	4.77	0.671	7.34	0.263	0.071	0.338	3.58	0.616
4.29	7.69	29.4	1.20	15.0	0.090	0.081	0.030	4.14	5.59	0.918	5.26	0.243	0.080	0.290	3.10	0.671
4.48	5.15	50.0	1.05	16.5	0.317	0.198	0.127	4.01	4.50	0.595	11.11	0.353	0.064	0.260	10.57	1.65

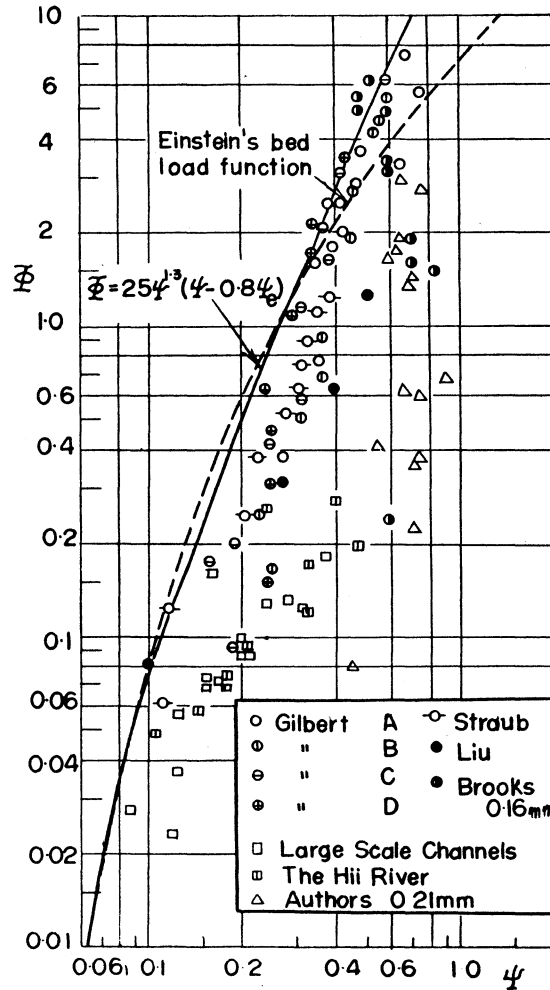


Fig. 5. The correlation between the intensity of transportation rate near the bed and the tractive force.

$$\Phi_0 = 25\Psi^{1.3} (\Psi - 0.8 \Psi_c) \quad (2)$$

with $\Psi_c = 0.0475$ as the value of dimensionless critical tractive force, while the curve E represents the Einstein's bed load function for the case of uniform grains and rough region. Both of these curves coincide each other in the region of bed load transport, but for $\Phi_0 \geq 0.2$ some considerable differences are seen between them. This comes from the fact that in Eq. (2) the suspended materials near the bed are also taken into account.

In Fig. 5 the data from Gilbert, H. K. Liu [9] and L. G. Straub [10] were obtained in the ordinary laboratory flume with moderate sands, where the large values of Ψ were attained by making the slope I large. Roughly speaking, they

may be represented by a single curve in the Φ — Ψ plane, although the experimental data are markedly scattered. On the contrary, in the large channel as well as in the Hii River, where the large values of Ψ were attained by making the water depth large with constant slope, the results of observations make their appearances differently. And further, from the results of experiments with fine sands no correlations can be seen between Φ and Ψ . considering that these data are concerned with the sand waves of considerable varieties in their scales and characters, we can understand the significant rôle of sand waves in the transportation rate.

As is mentioned already, Φ_0 is a function of Ψ only in the absence of sand waves at the bed. Accordingly, if we assume that the mechanism of sand movements on the rear side of sand wave is similar to that on the flat and even bed, we may determine experimentally the sheer stress τ_e which contributes to the sand movements, so long as we know the value of Φ in the presence of sand waves and use it in Eq (2) in place of Φ_0 . Referring τ_e as the effective tractive force hereafter, we shall make some considerations below on the expression of τ_e/τ_0 from the practical points of view.

Let us suppose the sand waves of length λ and of height H are formed at the bed composed of the sand grains of diameter D . Then from the dimensional considerations we can infer the functional relation:

$$\frac{\tau_e}{\tau_0} = f\left(\frac{H}{\lambda}, \frac{H}{D}\right)$$

Now, since H is almost equal to the equivalent roughness k_s of the flow and H/λ is closely related to k_s/H as will be seen in section 5, one of the most simple

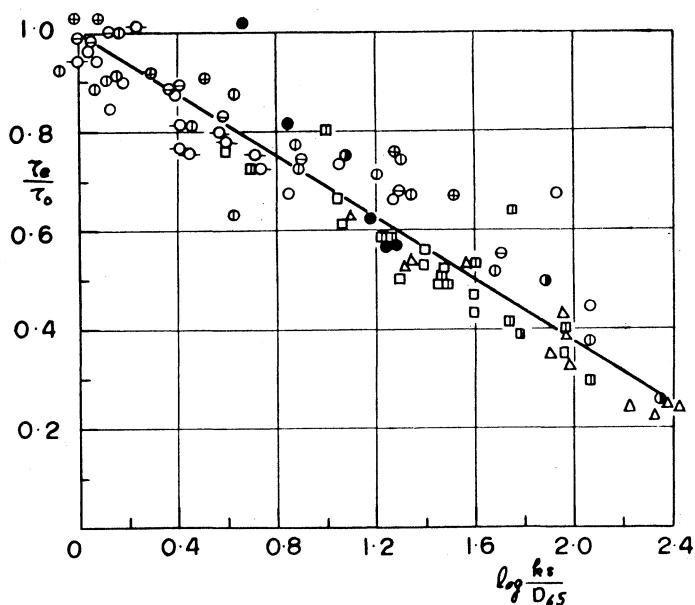


Fig. 6. Effective tractive force as a function of the equivalent roughness of flow.

method of taking into account the bed irregularities is that we consider τ_e/τ_o is likely to be expressed in terms of k_s/D . In Fig. 6 where τ_e/τ_o is plotted against $\log_{10} k_s/D$ from the experimental data in Fig. 5, we can see definitely the close correlation between these quantities, and the equation

$$\tau_e/\tau_o = 1 - 0.315 \log_{10} \frac{k_s}{D} \quad (3)$$

shown in the full line, is valid for $\tau_e/\tau_o \geq 0.2$

After the Einstein's theory, on the other hand, $\tau' = \rho g R' I$ determined by Eq. (1) corresponds to τ_e , and so we have the expression

$$\sqrt{\frac{\tau_e}{\tau_o}} = \sqrt{\frac{R'}{R}} = \frac{1}{1 + \frac{5.75}{\varphi} \log_{10} \frac{\tau_e}{\tau_o} + \frac{5.75}{\varphi} \log_{10} \frac{x k_s}{D_{65}}}$$

on rewriting Eq. (1). However, for the flow in open channels and rivers, the value of φ lie between 5–25, and when the influence of sand waves are significant in particular, they are confined within the narrow range covering 5–15. Besides, considering the fact that the second term in a denominator of the last side is less important than the third one, we may safely use a certain constant value of φ , 10 say, in the second term without causing any appreciable error. In other words, the Einstein's formula for τ' indicates that τ_e is expressed as a function of $\frac{1}{\varphi} \log_{10} \frac{x k_s}{D_{65}}$ approximately. The results of calculations are shown in Fig. 7,

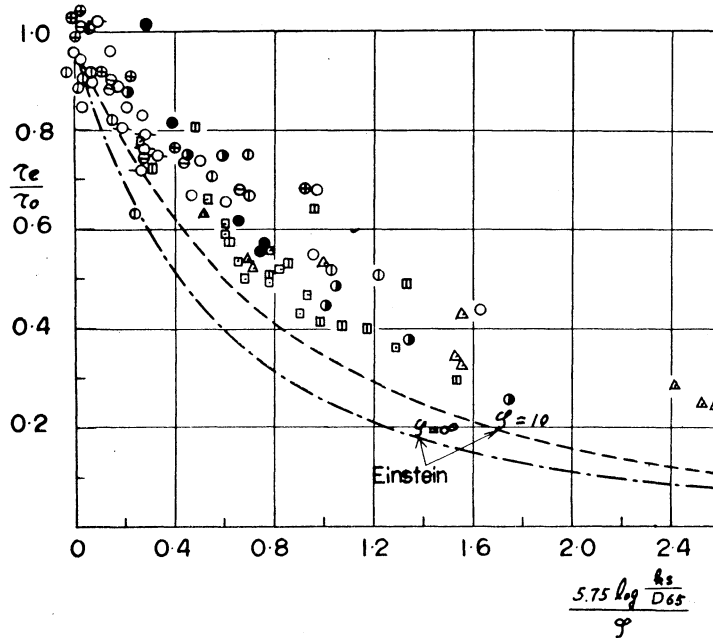


Fig. 7. Effective tractive force as a function of Einstein's parameter.

where the chain line and the dotted line correspond to the cases $\varphi = \infty$ and $\varphi = 10$ respectively, in the second term of the above equation. Although Eq. (1) tends to estimate the values of τ_e somewhat lower than the observed values, the qualitative coincidence seems to be satisfactory.

Lastly, the simplest experimental formula for the effective tractive force will be derived through the considerations which follow. When the water flows on the flat and even bed of hydraulic radius R with the mean velocity \bar{u} , the shearing stress τ_1 on the bed is given by

$$\frac{\bar{u}}{\sqrt{\frac{\tau_1}{\rho}}} = 6.0 + 5.75 \log_{10} \frac{R}{D_{65}} \equiv \varphi_0$$

As will be discussed in the subsequent paper, the sand movements are governed by the resistance of boundary layer developed along the rear sides of waves in the presence of sand wave and this resistance is nothing but the effective tractive force. Although their mechanism must be very complicated, it may be natural to assume that the coefficient of shearing stress at the rear side of sand wave is larger than on the flat bed on account of the effect of turbulence generated by waves themselves, and further that the rate of increase will depend upon the value of φ/φ_0 , that is,

$$\frac{\bar{u}}{\sqrt{\tau_e/\rho}} = \varphi_0 f\left(\frac{\varphi}{\varphi_0}\right),$$

from which we have

$$\frac{\tau_e}{\tau_0} = \frac{\varphi^2}{\varphi_0^2 \left[f\left(\frac{\varphi}{\varphi_0}\right) \right]^2}.$$

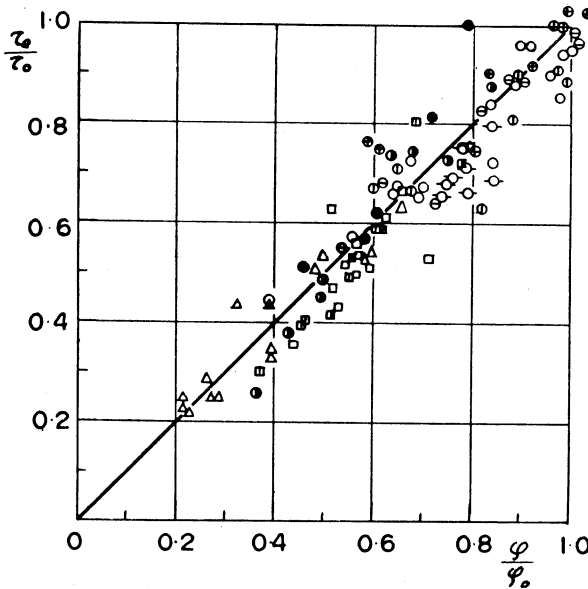


Fig. 8. Effective tractive force as a function of the coefficient of flow resistance.

The relation between τ_e/τ_c and φ/φ_0 is plotted in Fig. 8, showing the very simple expression

$$\frac{\tau_e}{\tau_c} = \frac{\varphi}{\varphi_0} \quad (4)$$

is appropriate.

Since the accuracies of Eqs. (3) and (4) are almost equal, it will be convenient to use Eq. (4) in practice for simplicity's sake. Thus the intensity of the transportation rate near the bed will be given by

$$\begin{aligned} \Phi &= 25 \Psi_e^{1.3} (\Psi_e - 0.8 \Psi_c) \\ \Psi_e &= \Psi \frac{\varphi}{\varphi_0} \end{aligned}$$

4. Characteristics of sand waves. As an instance of field observations let us begin with the description of the aspects of sand waves observed in the large scale channels. When the depth of water comes to about 6 cm, the finer grains begin to move and are sorted to form the sand waves of about 1 m in length and about 1 cm or lower in height. As the depth, and hence the tractive force, increase the coarser grains also set in motion in turn and the waves grow up more and more both in length and height. Each individual grain moves up along the rear side, rolling, sliding or making short hops and then tumbles down in a stratum from the crest into the vortices of the dead water region along the steep slope of about 33° at the lee side. Then the smaller parts of the grains are transported again to the rear side of the antecedent wave, being lifted by the local flow due to the periodic collapse of the vortices, and others are buried under the surging wave. Repeating these processes continually, the waves themselves advance slowly downstream with the velocity of about 0.1 cm/sec.

The sand waves with 0.21 mm grains in the flume, on the other hand, take a quite different course of development, that is, with the increase of the discharge the waves, being flattened out, disappear, and the bed becomes smooth again.

In the followings, we shall consider the typical characters of sand waves to some extent.

(a) Scale of sand waves.

Lately A. G. Anderson [3] has obtained theoretically the relation between λ/h and the Froude number in the form

$$2\pi \frac{h}{\lambda} \left[\tanh 2\pi \frac{h}{\lambda} - \frac{2}{\sinh 4\pi \frac{h}{\lambda}} \right] = \frac{1}{Fr^2} \quad (5)$$

on the basis of the idea that the surface wave is the cause of bed undulations. This equation, however, cannot reproduce our experimental results in the Hii River and the channel. For instance, the value of λ/h given by the above equation are 0.6–1.9 for the Froude numbers of 0.3–0.5, whereas the observed values in the channel are 3.5–9.8 for the same Froude number range.

Now, from the dimensional considerations the functional relations of the wave height and the wave steepness are inferred as

$$\frac{H}{h} \text{ and } \frac{H}{\lambda} = f\left(\psi_e, \frac{\bar{u}}{\sqrt{gh}}, \frac{\sqrt{\tau_e/\rho} D}{\nu}, \frac{h}{D}, \beta\right), \quad (6)$$

where ν is the kinematic viscosity of water and β is the dimensionless parameter representing the non-uniformity of the bed materials. For the convenience of practical use, let us further rewrite these parameters like

$$\frac{\bar{u}}{\sqrt{gh}} = \varphi\sqrt{I}, \quad \frac{\sqrt{\tau_e/\rho} D}{\nu} = \varphi_e^{\frac{1}{2}} \sqrt{sg D^3} / \nu \propto \varphi_e^{\frac{1}{2}} \left[\left\{ \frac{s}{1.66 \cdot 980} \frac{g}{(100\nu)^2} \right\}^{\frac{1}{3}} D \right]^{\frac{3}{2}}$$

$$\frac{h}{D} = \psi_e \frac{\varphi_0 s}{\varphi I}$$

where φ may be considered as a function of H/h , as H/h is closely related to k_s/h . Thus, in the case of uniform sand ($s = \text{constant}$), (6) becomes

$$\frac{H}{h} \text{ and } \frac{H}{\lambda} = f(\psi_e, I, D_n) \quad (7)$$

where D_n defined by $D_n = \left\{ \frac{s}{1.66 \cdot 980} \frac{g}{(100\nu)^2} \right\}^{\frac{1}{3}} D$ is the dimensionless representation of grain diameter of sands.

The measured values of wave height H/R_b and wave steepness H/λ are plotted against $\psi_e = \psi \frac{\varphi}{\varphi_0} = \frac{R_b I}{s D} \frac{\varphi}{\varphi_0}$ in Fig. 9 and Fig. 10 respectively, in which

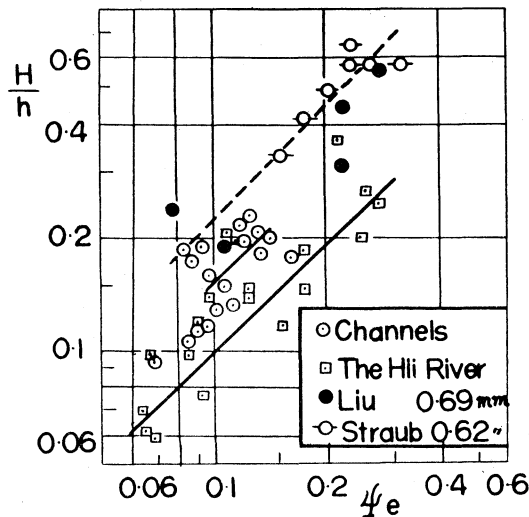


Fig. 9. Wave height. (coarse sand)

we are concerned with the case of coarse sands whose diameters are larger than 0.6 mm. To be noticed, H/R_b increases with Ψ_e almost linearly, showing, however,

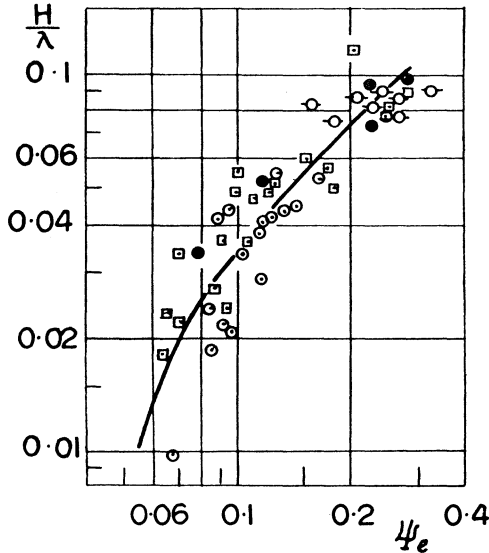


Fig. 10. Wave steepness. (coarse sand)

systematic deviations according as the width of channels, that is the values of H/R_b , are largest in the flumes, medium in the large scale channels and smallest in the Hii river. This fact may be explained in the following way. When the vortex tubes, formed at the trough of the sand wave, reach the side wall, they will cause the local scour near the wall. And we can suppose that the narrower the channels, the more remarkable may be the influence of this scouring action. The wave steepness $\frac{H}{\lambda}$ increases with Ψ_e too, and seems to have a tendency to settle in the final state.

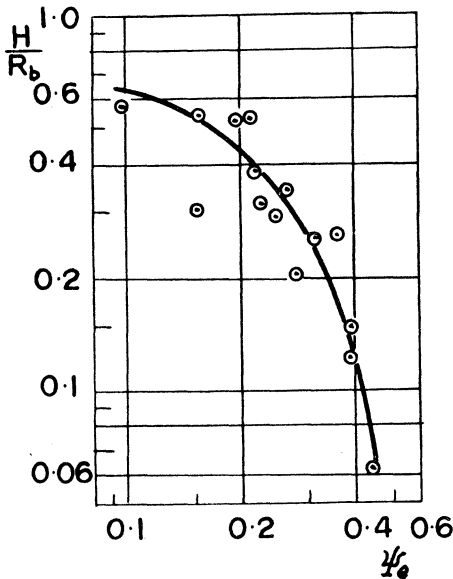


Fig. 11. Wave height. (fine sand)

Fig. 11 shows the relation in very contradistinction to the foregoing coarse sands, H/R_b decreases with increase of Ψ_e , although the range of Ψ_e is almost the same for both cases. What does this mean? According to Eq. (7), H/R_b depends not only on Ψ_e but on the slope I and on the grain-diameter D_n as well. At present however, the effects of I and D_n cannot be separated experimentally, as only few observation has been made in these connexions. It may be natural to suppose that the Froude number (or the slope I) is one of the important factors relating to the transition from a dune to a smooth bed or from a smooth bed to an antidune, but in view of the fact that some of the experimental results with coarse sands (due to Liu and Straub) and some with fine sands (due to the

present authors) correspond to the approximately same values of I , we are suggested that such largely different characters of sand waves as mentioned above are likely to the grain-diameter of bed materials. Let us consider below the state of affairs in some details.

As is well known, the sediment load has been divided into two classes, the bed load and the suspended load, according as its mode of movement. And, when Ψ_e exceeds the limit Ψ'_s , which is to be determined by D_n (Appendix; Fig. 2), the suspended load becomes significant. (See Appendix.) The value of Ψ'_s is nearly constant and equals about 0.7 for $D_n > 0.05$, but decreases abruptly with the decrease of D_n beyond 0.05. For instance, when D_n is 0.02, Ψ'_s is 0.24 only. Accordingly, even for the given same values of Ψ_e , there may be an essential difference concerning whether the suspended load is negligibly small or it is predominantly large, according as the grain-diameter of bed materials. If the vigorous exchange of sand grains proceeds between the bed layer and the turbulent region above it, the sand waves will hardly maintain their shape. Thus, we may say that the sand waves tend to break down when the suspended load is dominant, while they tend to develop when the bed load is dominant.

(b) The relation between the scale of sand wave and the transportation rate.

Denoting the deviation of the bed profile measured from the reference line by η , we have the equation

$$\frac{\partial \eta}{\partial t} + \frac{I}{I-\epsilon} \frac{\partial q_B}{\partial x} = 0,$$

where q_B represents the bed load and ϵ is the porosity of deposits.

On the other hand, if we can assume that the shape of sand waves does not change appreciably for a sufficient long time, we have

$$\frac{\partial \eta}{\partial t} + u_r \frac{\partial \eta}{\partial x} = 0.$$

Supposing that $\eta=0$ corresponds to the trough of waves where the transportation is q_0 , η is thus connected with the distribution of transportation rate along the rear side of the wave: that is,

$$\eta = \frac{I}{I-\epsilon} \frac{q_E - q_0}{u_r}.$$

Consequently, the mean transportation rate \bar{q}_B per one wave-length is

$$\bar{q}_B = \frac{Hu_r \alpha (I-\epsilon)}{2} + q_0, \quad (8)$$

where α is the shape factor of the profile of sand waves with which the volume per unit width of a single wave-length is expressed as $H\lambda\alpha/2$. At the trough of asymmetrical sand wave with steep lee-side, sand grains are moved only by the action of local flow due to the collapse of vortices in the dead water region. Since q_0 is accordingly supposed to be small, we can infer from Eq. (8) that the

bed load is nearly equal to the rate of collective movement in the form of sand wave as a whole.

Fig. 12 shows the relation between $H \cdot u_r$ and the transportation rate measured in the Hii River and the large scale channels. By means of a simple method ϵ has been found to be 0.46, and the shape factor α has been obtained by integrating the measured bed profile covering some 5–10 successive waves for several

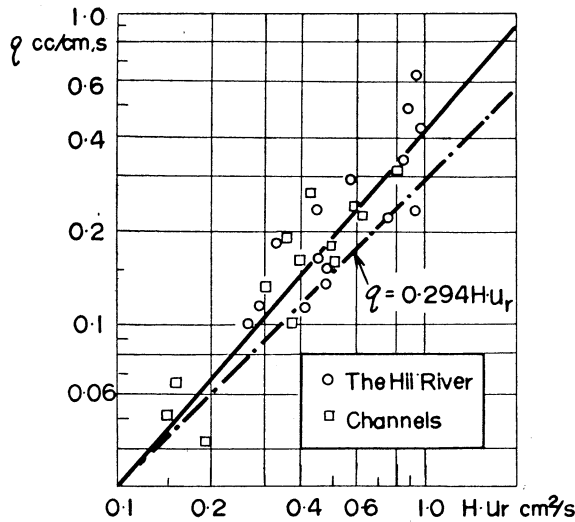


Fig. 12. The relation between the bed load and the scale of sand waves.

wave height. We have had, in this way, the value of $\alpha = 1.13$ in the Hii River and 1.09 in the channels. So substituting $\alpha = 1.10$ and $\epsilon = 0.46$, Eq. (8) becomes

$$\bar{q}_B = 0.294 H u_r + q_0. \quad (9)$$

The chain line in Fig. 12 corresponds to the case of $q_0 = 0$ in the above equation. Although the measured points scatter considerably, it may be noticed that they lie above the dotted line. The ratio q_0/\bar{q}_B , whose value is nearly zero at the low transportation rate and is 0.29 at $\bar{q}_B = 0.42$ cc/cm sec ($\Psi_B \doteq 0.3$), seems to increase with Ψ_e , indicating that the individual sand grains are exchanged continually. Further, Liu [9] has reported that the transportation rate coincides with the collective movement in the flume experiments with 0.69 mm sands. From these facts, we are able to estimate the degree of the bed load at once by measuring the scale and the advance velocity of the sand waves in the rivers with asymmetrical sand waves. Considering the difficulties accompanying in the measurements of bed load at the actual rivers, this method seems to be of great practical importance.

In the flume experiments with 0.21 mm sands, we could not establish the relation between $H \cdot u_r$ and q_B . In the case of fine sands, Eq. (8) does not hold;

probably the principal reason of it is that then the shape of sand waves changes continually.

(c) Advance velocity of the sand waves.

Up to the present, various experimental formulas have been proposed, in which the advance velocity u_r of sand waves is expressed in terms of the mean velocity \bar{u} of flow. Nevertheless, our field observations show little relation between u_r and \bar{u} , so it seems to the authors that u_r must be governed not only by the mean velocity of flow but by the transportation rate and the scale of sand waves.

As has been already mentioned, the essential feature of sand wave is the collective transport of bed materials, and in the case of coarse sand, \bar{q}_B is nearly proportional to Hu_r . Furthermore, considering that H/R_b is mainly related to Ψ_e and D_n and $q_B/\sqrt{sgD^3}$ is a function of Ψ_e , the dimensionless wave velocity $u_r R_b / \sqrt{sgD^3}$ also may be expressed as a function of Ψ_e and D_n . As the case of coarse sands, the experimental results obtained by Liu [9] in the flume and by the present authors in the Hii River and channels are plotted in Fig. 13. To be worth

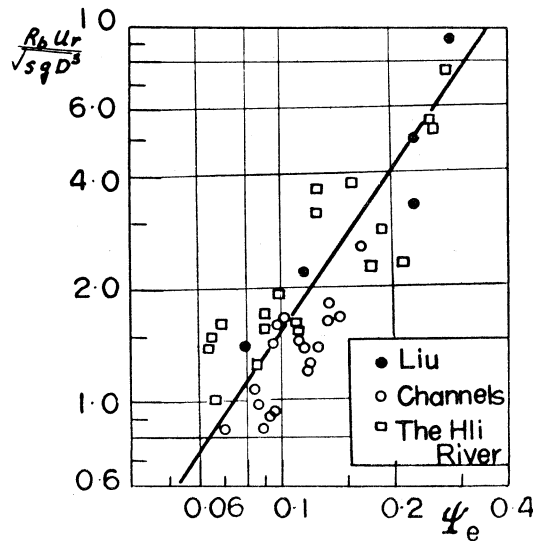


Fig. 13. Advance velocity of sand waves. (coarse sand)

noting, these data obtained under the different hydraulic conditions of flow can be represented by a single curve. The experimental results with fine sands, on the other hand, are found in Fig. 14. The observed points of 0.10 mm sands obtained by N. H. Brooks [11] show some systematic deviation, giving a little smaller velocities than others, but as a general tendency it may be seen that the advance velocity u_r of fine sands increases more rapidly than that of coarse sands. The full lines in Fig. 13 and Fig. 14 correspond to the simple empirical formulas

$$\frac{u_r R_b}{\sqrt{sg D^3}} = a \psi_e^m \quad (10)$$

for the advance velocity of sand waves, where $a=48.6$, $m=1.5$ for coarse sands ($D_n \geq 0.06$) and $a=76.1$, $m=2.5$ for fine sands ($D_n = 0.01-0.021$) respectively. Strict-

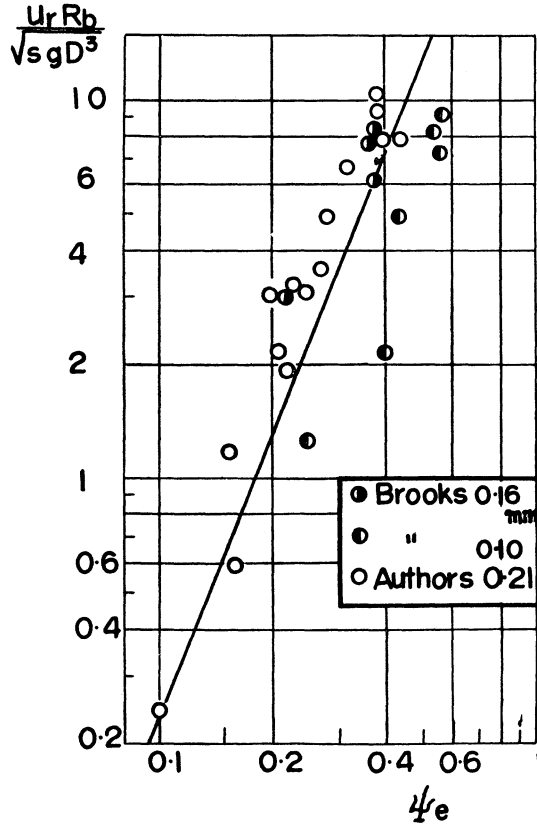


Fig. 14. Advance velocity of sand waves. (fine sand)

ly speaking, the exponent m and dimensionless number a in above equation may be considered as functions of D_n . However, when the bed is composed of the coarse sands, we can suppose m and a take constant values and Eq. (10) is rewritten as

$$\frac{u_r}{u_*} = \frac{48.6}{s} I \left(\frac{\varphi}{\varphi_0} \right)^{1.5}, \quad (11)$$

which tells us that in the rivers with negligible suspended load the ratio of advance velocity of sand waves to shear velocity is proportional to the slope I nearly independently of grain diameter and decreases with increase of the wave-height as the result of decrease in (φ/φ_0) .

5. The resistance law of rivers with sand transport. The main difference between the resistance laws of stream for the rivers with sand transport and for those with fixed bed originates from the fact that in the former case the bed irregularities such as sand waves change their scale according to the hydraulic conditions of flow and bed materials, while in the latter case, on the contrary, the scale of roughness does not depend on these hydraulic conditions. Formerly, one of the present authors [12] obtained, from these points of view, the relationship between the equivalent roughness of the flow and the tractive forces, with use of the data in Japan and in Manchuria, whereas from the measurements in the American rivers. H. A. Einstein and N. L. B. Barbarossa [13] found that bar resistance $\bar{u}/\sqrt{gR'I}$ were expressed by $sD/R'I$. However, the results of these two studies are contradictory each other; that is, with the increase of the dimensionless tractive force, the resistance coefficient given by the former theory increases, but that given by the latter one decreases. Thus, we must say that both of them grasp only one side of the complicated nature of sand waves, the other side being overlooked altogether.

Succeeding the previous section, where the scale of sand waves formed at the bed has been discussed, we shall describe in this section the relation between the equivalent roughness of flow and the scale of sand waves, and further some considerations will be made on the resistance of the rivers with sand transport in this connexion.

(a) The relation between the scale of sand waves and equivalent roughness of the flow.

We have studied the equivalent roughness of flow with artificial fixed bed

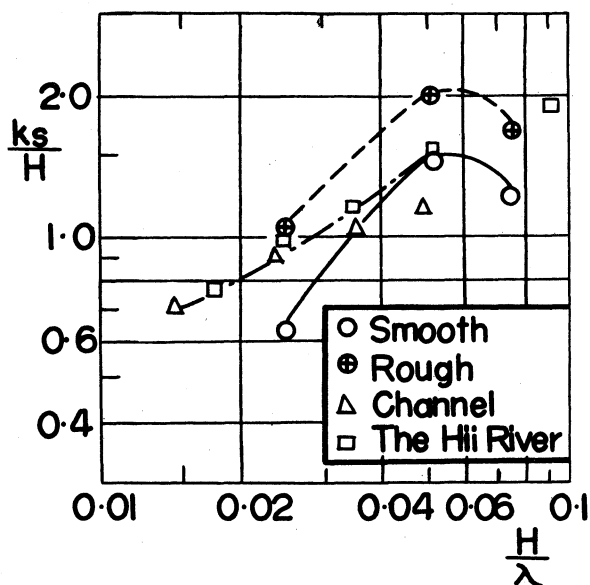


Fig. 15. Equivalent roughness of flow as the function of wave steepness.

undurians in the laboratory as well as the field works at the Hii River and the channels. As will be described fully in the subsequent paper, the flume experiments have been made for three kinds of the wave-steepness (1 cm in wave-height commonly, and 40, 20, 13.5 cm in wave-length respectively). And further, in order to check the effect of surface roughness of sand waves, the bed surface has been made rough by covering it with uniform sand of 0.21 cm grain diameter, in comparison with the smooth case. The values of k_s/H obtained by field observations* together with those for artificial waves are plotted against the wave-steepness H/λ in Fig. 15.

It can be seen that the values of k_s/H increase with H/λ for $H/\lambda > 0.05$, reaching the maximum at $H/\lambda = 0.05 \sim 0.074$. The change of k_s/H with H/λ are similar to, though more gentle than, the results for two dimensional rectangular roughness summarized by J. W. Johnson [14]. Roughly speaking, at the range of practical importance, the equivalent roughness of the flow over the sand waves is in the same order of magnitude with the height of the waves.

(b) The resistance law of rivers with movable bed.

It has been shown in section 4 that the scale of sand waves formed at the bed are expressed as

$$\frac{H}{h} \text{ and } \frac{H}{\lambda} = f(\Psi_e, I, D_n, \beta).$$

Now, since k_s/H is determined mainly by H/λ , the functional form of φ defined

Table. 4 Summary of data on rivers with sand transport.

river	grain diameter		mean slope	water depth
	$D_{35}(\text{mm})$	$D_{85}(\text{mm})$	$I \times 10^3$	h (cm)
○ channels	0.95	1.96	1.66	10-45
⊕ Hii	1.02	1.82	1.20	20-100
● Hii (b)	0.69	1.46	0.99	25-86
◐ Kimotsuki	0.53	1.57	0.62	112-154
◑ Kimotsuki	0.57	1.01	0.20	101-282
⊖ Hun	0.85	3.60	1.25	37-105
△ Shirakawa	0.21	0.30	0.53	56-230
△ Hun	0.21	0.24	0.54	32-119
□ Missouri	0.16	0.21	0.169	182-288
▢ Bis Sioux	0.32	0.46	0.189	111-408
■ Platte	0.32	0.58	0.738	55-167
▣ Elkhorn	0.20	0.28	0.528	46-202
▤ Salinas	0.39	0.67	1.16	21-97
-○- Salinas	0.70	1.87	1.72	14-102

* As the observed points are fairly scattered, individual values of k_s/H are averaging over the proper range of H/λ .

by the logarithmic formula for mean velocity $\bar{u}/u_* = 6.0 + 5.75 \log_{10} \frac{h}{k_s}$ will be expressed as

$$\varphi = f(\Psi_e, I, D_n, \beta), \quad (12)$$

except near the critical tractive force. Although it is very difficult to determine the functional form of Eq. (12) in such a manner as to cover the case of experimental flume as well, the following simplifications may be allowable for many rivers with moveable beds. That is, φ may be considered as the function of Ψ_e and D_n in an approximate way, so instead of (12) we have

$$\varphi = f(\Psi_e, D_n). \quad (13)$$

The reasoning is like this: K. Aki [15] and E. Yatsu [16] have studied the longitudinal variation of the grain-diameter composing the bed along the several rivers in Japan and found that there exists the correlation between the grain-diameter and the slope of the rivers. Referring to the mean surface slope and

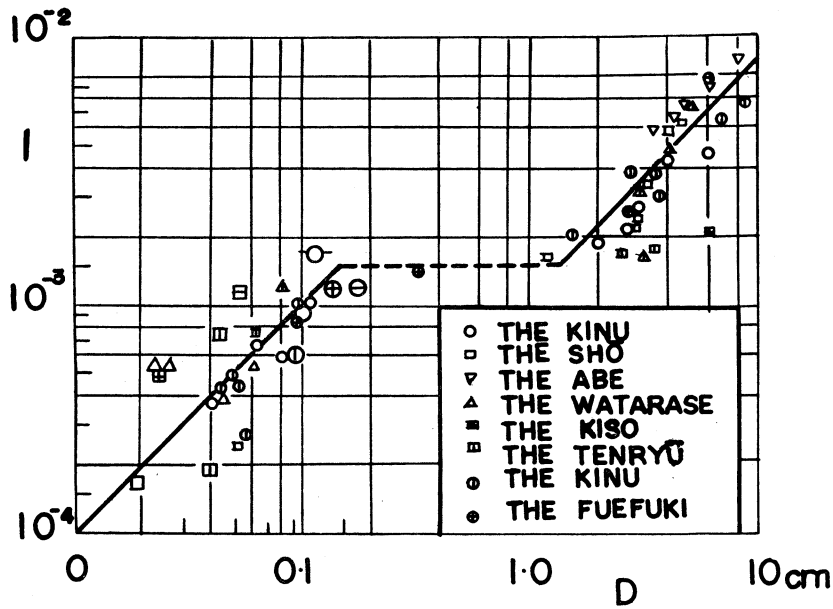


Fig. 16. Correlation between the slope of the rivers with movable beds and the grain diameter.

$D = \sqrt{D_{35} D_{65}}$, their results are shown in Fig. 16 which contains also the data of the rivers in Table 4. Besides, S. Awazu [17] has pointed out that the grain-diameter of the bed materials has some correlation with Sakai's parameter β which

is related to Kramer's M through $\beta = \frac{2+M}{1+2M}$.

From these facts, we can assume that there exist mutual dependencies be-

tween I , D_n and β statically in the rivers with movable bed. Accordingly (12) may be reduced to (13).

Lets us now find out this functional from of φ from the data summarized in Table 4 and our results of observations at the Hii River and the channels. To be noted, the data at the Hii River (b) were obtained by K. Kikkawa [18], those at the Kimotsuki river by M. Araki [19], those at the Hun-ho by S. Nagai [20] respectively, and the data concerning the American rivers are taken from "the river channel roughness" by Einstein Barbarossa [13].*

Fig. 17 shows the relation between φ and Ψ_e . Though the observed points are largely scattered, it is likely to be seen that first φ decreases with the increase of

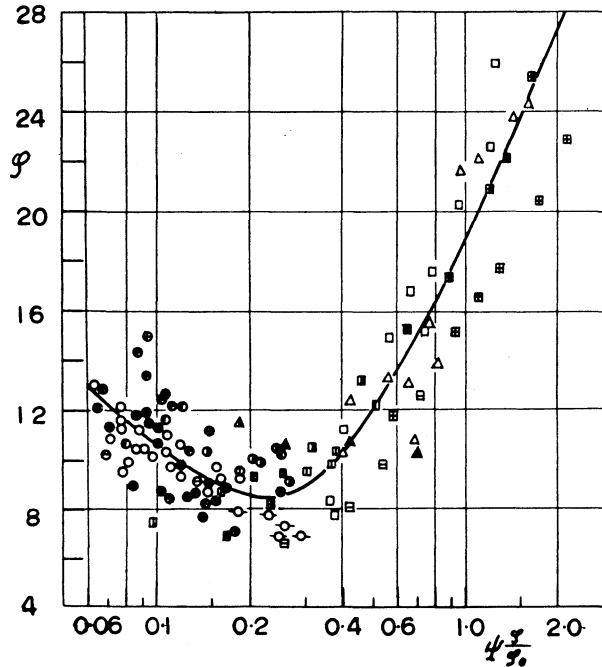


Fig. 17. Mean velocity of the rivers with movable beds as a function of effective tractive force.

Ψ_e for $\Psi_e \leq 0.2$ and then increase for $\Psi_e \geq 0.3$, being minimum at $\Psi_e = 0.25$. As has been already mentioned, however, the process of development of sand waves differs considerably according as the grain-diameter of bed materials, so that we shall add a few words on the effect of D_n shown in Fig. 17. Of the rivers cited Table 4, most of American rivers, the Hun-ho (at Shenyang) and the Shirakawa correspond to the case of fine sands. In these rivers, φ increases with Ψ_e , the rate of increase being large at $\Psi_e \geq 0.4$. This fact is consistent with our experimental results with 0.21 mm sands that the sand waves of fine grains tend to be in the

* We are grateful to the courtesy of Dr. Einstein about these data.

process of breakdown with Ψ_e . On the other hand, it has been observed that the sand waves of coarse grains tend to develop with increase of Ψ_e . Correspondingly, φ decreases with Ψ_e there, contrary to the above case. It must be noted that the behaviour of sand waves, developing or breaking down, is a true reflection of the resistance law of rivers with the sand transport.

6. Summary. The main conclusions drawn from our present investigations together with the available existing experimental data can be summarized as follows:

- (1) A strong influence of sand waves upon the transportation rate in channels and rivers becomes clear now, and an empirical formula for the transportation rate in the rivers of bed load type is proposed where the practical parameter representing the ratio of the effective tractive force to the total stress on the bed as function of bed irregularities is introduced.
- (2) The development of sand waves proceeds fairly differently according as the grain diameter of bed materials; that is, in the case of coarse sands transported after the bed load type, sand waves grow up in their scale with the increase of the effective tractive force Ψ_e . Whereas, in the case of fine sands containing the considerable quantities of suspended load, sand waves are flattened out already for the same range of Ψ_e .
- (3) For coarse sand the rate of collective movements in the form of sand waves is approximately equal to the bed load, and the dimensionless expression of the advance velocity is obtained.
- (4) The equivalent roughness of the flow is closely related to the scale of sand waves, its value being nearly equal to the wave-height.
- (5) The value of the mean velocity φ in the rivers with sand transport is expressed in terms of Ψ_e and the grain diameter as well, which is a reflection of the fact stated in (2) above.

The authors are grateful to Hii River Construction Office, Ministry of Construction, Japan, for kindly aids in the field observations. Further, their thanks are also due to Messrs. S. Ikeda, K. Susuki and T. Saitō who helped them in experimental side and in the related desk work.

Appendix

Types of sand transport in the rivers.

When the tractive force of the flow exceeds a certain magnitude (i. e. the critical tractive force as it is called), sand grains at the bed begin to move after the bed load type, and then as the tractive force increases further, there appears the transport after the suspended load type too, whose proportion to the total load also increases more and more. In detail, however, the transport of suspended load type makes its appearance differently according as the grain diameter of

sands. Namely, for fine grains the concentration of *suspended load* becomes approximately uniform owing to the active diffusion, but for coarse grains, on the contrary, the *suspended load* localizes upon the layer near the bed only. In the former case, where the suspended load dominates, the suspended load sampler may be of use, while in the latter case, where the suspended load and bed load are comparable, the load measurement is very difficult. Furthermore, theoretical estimation of the suspended load is not so reliable altogether because of various errors in the determinations of diffusion coefficients and the lower limit concentration of suspended load. In channel experiments, on the other hand, it has been usual to observe the total load itself without separating it into bed and suspended loads, and we have already a fair number of these experimental data now. Thus, the practical standard of classifying the mode of transport is eagerly awaited besides the theoretical one, so that the comparison between channel experiments and actual river observations may be possible.

It may be quite reasonable to suppose that the bed load would be caught by the turbulent eddies to suspend in the flow when the sand motion due to turbulence becomes comparable with the sedimentation velocity v_s in magnitude. Denoting by ν the root mean square of vertical turbulent velocities, this condition can be formulated simply as $\nu = v_s$, since the motion of sand in the turbulent field is found to be nearly equal to that of turbulence, so long as the scale of turbulence is large enough compared with the grain diameter [21].

Now, according to Professor Kurihara [22], the intensity of turbulence ν is related to the friction velocity u_* in such a manner as

$$\nu = \sqrt{\frac{2}{0.256(1+\alpha^2+\beta^2)}} u_* ,$$

where α and β mean the ratios of root mean squares of turbulent velocities to ν in the parallel and the perpendicular directions of flow respectively. Assuming $\alpha=2.4$ and $\beta=1.5$ with the reference to the measurements of turbulence between parallel plates, the above relation becomes.

$$\nu = 0.93 u_* .$$

By the way, supposing that the distribution of turbulent velocities obeys the normal error law, the probability of occurring the velocities larger than ν would be 32%, and hence the criterion $\nu = v_s$ would correspond to the period where a certain quantity of suspended load can be already observed. Let now Ψ'_s be the tractive force at this period, then we have

$$\Psi'_s = (F/0.93)^2 , \quad (a)$$

where $F = v_s / \sqrt{sgD}$ which is function of the dimensionless grain-diameter D_n , and so Ψ'_s also depends on D_n . The chain line in Fig. 1 shows Ψ'_s calculated from the Rubey's empirical formula

$$F = \sqrt{\frac{2}{3} + \frac{36 \nu^2}{gsD^3}} - \sqrt{\frac{36 \nu^2}{gsD^3}} .$$

It will be seen that when $D_n > 0.05$, Ψ'_s is roughly constant (about 0.7) and that

for smaller D_n , Ψ'_s sharply decreases with D_n .

Thus, when Ψ exceeds Ψ'_s , the total load q contains both the bed and the suspended loads simultaneously, and in absence of sand waves q can be expressed in Einstein's representation [7] as.

$$\begin{aligned}\phi &= \frac{q}{\sqrt{sgD^3}} = \frac{q_B}{\sqrt{sgD^3}} + \frac{11.6u_* C_a a}{\sqrt{sgD^3}} (PI_1 + I_2) \\ &= \frac{q_B}{\sqrt{sgD^3}} \left\{ 1 + \beta(PI_1 + I_2) \right\}.\end{aligned}\quad (b)$$

In this equation, C_a is the concentration at $y=\alpha D$, P is function of h/D , I_1 , and I_2 are function of $A = \frac{\alpha D}{h}$ and $Z = \frac{v_s}{ku_*}$, and β and α are dimensionless quantities depending on the physical conditions near the bed only not on the parameter h/D .

An important difference between the sand transport in experimental channels and in actual rivers is that the same value of tractive force corresponds to shallow depths and steep slopes in channels and vice versa in rivers, the value of h/D being largely different; that is, under the usual conditions D/h is of order 10^{-2} in channels while it is of order 10^{-3} or 10^{-4} in rivers. On the other hand, noting that in (b) $q_B/\sqrt{sgD^3}$ is a function of Ψ , I_1 , and I_2 are functions of $Z = v_s/0.4u_* = F\Psi^{-1/2}/0.4$ and D/h , the quantity $q/\sqrt{sgD^3}$ is found to be a function of Ψ , D_n and D/h . Therefore, for given tractive force Ψ and bed material, the only parameter which can destroy the similarity of total loads in channels and rivers must be D/h . But since no other terms than $[PI_1 + I_2]$ are influenced by this parameter D/h , the effect in question is well represented by calculating $PI_1 + I_2$ as is shown in Fig. 1, where, making use of Einstein's value $\alpha = 2(A = 2D/h)$, the cases $A=10^{-2}$ (in channels), $A=10^{-3}$ and $A=10^{-4}$ (in rivers) are illustrated. To be clearly seen in this figure, the values of $[PI_1 + I_2]$ (relative to that for $A=10^{-2}$) are almost independent of A for $Z \geq 1.5$, but largely affected by A for $Z < 1.0$. This is, of course, a reflexion of the fact that when Z is large the suspended load concentrates near the bed, being almost independent of the depth, and as Z diminishes the diffusive action extends to the upper layer, the concentration being more and more uniform over the cross-section,

In conclusion, it is the value of Z which decides whether the rôle of D/h in the suspended load, and accordingly in the total load, can be neglected or not. Assuming $Z=1.5$ as the critical value for definiteness' sake, the intensity of total load ϕ would be expressed as a function of bed load parameters only, so long as the tractive force Ψ is small than Ψ_s which is to be obtained from

$$\frac{v_s}{0.4u_*} = \frac{F\Psi_s^{-1/2}}{0.4} = 1.5.$$

Ψ_s is a function of D_n , and as the full line in Fig 2 shows, it is like Ψ'_s nearly constant for $D_n \geq 0.05$ and sharply falls off for smaller D_n .

In the presence of bed undulations, however, boundary layer will develop along the bed (as will be described in the subsequent paper), and so the suspended load inside the boundary layer together with the bed load will be governed not by Ψ but by Ψ_e representing the boundary layer stress. Consequently when the sand waves are present, the above argument would require some corrections, but provided that $\Psi_e \leq \Psi_s$, we may approximately suppose Φ is independent of h/D .

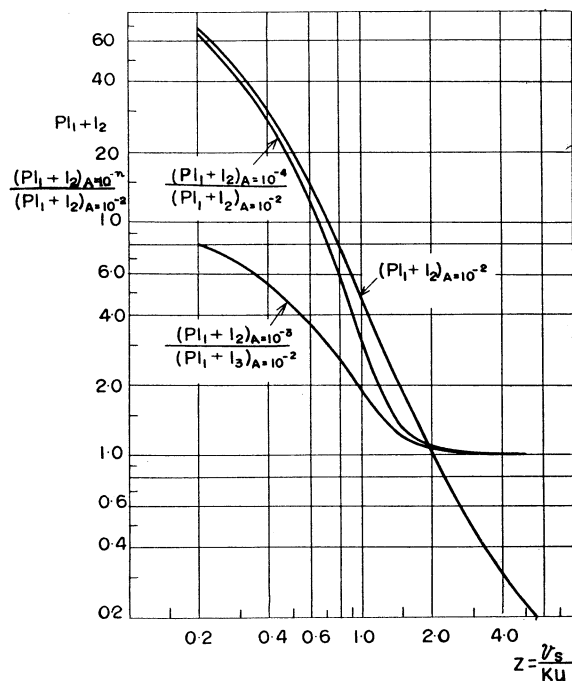


Fig. 1. $(PI_1 + I_2)$ as the function of Z and h/D .

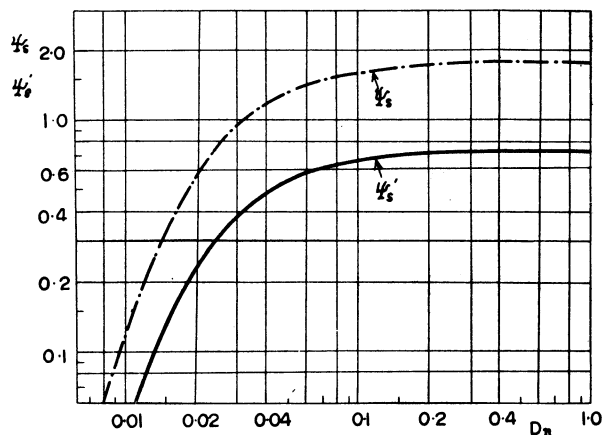


Fig. 2. Effect of the grain diameter on the criterion of bed load type transport.

From these points of view, the actual rivers will be classified into the bed load type and the suspended load type according as the effective tractive force Ψ_e is smaller or larger than Ψ_s specified by D_n . For rapid rivers with coarse sands, such as many of the Japanese rivers, this classification is very convenient in practice.

References

- [1] G. K. Gilbert, "The Transportation of Debris by Running Water." U. S. Geological Survey, Prof. Pap. 86, 1915
- [2] S. Leliavsky, "An Introduction to Fluvial Hydraulics." 1955, p. 27
- [3] A. G. Anderson, "The Characteristics of Sediment Waves Formed by Flow in Open Channels." Proc. Third Midwestern Conf. on Fluid Mechanics, 1953
- [4] H. K. Liu, "Mechanics of Sediment-Ripple Formation." Proc. A. S. C. E., vol. 83, No. Hy2, 1957
- [5] T. Tsubaki, T. Kawasumi and Y. Yasutomi, "On the Influences of Sand Ripples upon the sediment Transport in Open Channels." Rep. of Res. Inst. for App. Mech., Kyūshū Univ., vol. 2, No. 8, 1953
- [6] H. A. Einstein, "Formulas for the Transportation of Bed Load." Trans. A. S. C. E., vol. 107, 1942
- [7] H. A. Einstein, "The Bed Load Function for Sediment Transportation." Technical Bulletin, No. 1026, U. S. Dept. of Agriculture, 1950
- [8] T. Tsubaki, "On the Transportation of Sands in the Open Channels." (in Japanese), Rep. of Res. Inst. for Fluid Eng., Kyūshū Univ., vol. 7, No. 4, 1951
- [9] H. R. Liu, Discussion of N. Chien, "The Present Status of Research on Seaiment Transport." Trans. A. S. C. E., vol. 121, 1956, p. 877
- [10] L. G. Straub, Discussion of H. Kramer, "Sand Mixtures and Sand Movement in Fluvial Models." Trans. A. S. C. E., vol. 61, 1935, p. 668
- [11] N. H. Brooks, "Mechanics of Streams with Movable Beds of Fine Sand." Proc. A. S. C. E., vol. 81, Sep. No. 668, 1955
- [12] T. Tsubaki and A. Furuya, "On the Resistance Law of Rivers with Transportation of Sands." (in Japanese), Rep. of Res. Inst. for Fluid Eng., Kyūshū Univ., vol. 7, No. 4, 1951
- [13] H. A. Einstein and N. L. Barbarossa, "River Channel Roughness." Proc. A. S. C. E., vol. 77, Sep. No. 78, 1951
- [14] J. W. Johnson, "Rectangular Artificial Roughness in Open Channels." Trans. Ame. Geophy. Union, vol. 25, 1944
- [15] K. Aki, "Kasō-ron" (Theory of River Aspect.) 1951

- [16] E. Yatsu, "On the Longitudinal Profile of the Graded River." Trans. Ame. Geophy. Union, vol. 36, 1955
- [17] S. Awazu, "Few Properties of Bed Material, and its Application." (in Japanese), Trans. Japan Soc. of Civ. Eng., No. 36, 1956
- [18] H. Kikkawa and Y. Sone, "A Method to Design Channel Section of the Alluvial River." (Report on the Research for the Fundamental Problems to improve the River Hii), Rep. of P. W. Res. Inst. Min. Const., vol. 85, 1953
- [19] M. Araki, "Some Considerations on the Equilibrium of Beds along the Kimotsuki River." (in Japanese), Rep. of the 6th. Annual Meeting of Res. on Const. Works, Min. of Const., 1953.
- [20] S. Nagai, "Idōkashō o yūsuru Suiro oyobi Shizen-kasen ni okeru Shin Ryūsoku-kōshiki." (A New Velocity Formula of Rivers and Channels with Movable Bed.), Jour. of Civ. Eng. Soc. of Japan, vol. 28, No. 5 and 7, 1942
- [21] T. Tsubaki "On the Motion of Sediments in the Turbulent Fields." Rep. of Res. Inst. for Fluid Eng., Kyūshū Univ., vol. 7, No. 4, 1951
- [22] M. Kurihara, "Investigations on Turbulence (4). On Turbulent Viscosity." Rep. of Res. Inst. for Fluid Eng., Kyūshū Univ., vol. 3, 1947

(Received March 5, 1959)